0026-895X/11/7903-368–380$20.00
MOLECULAR PHARMACOLOGY
Vol. 79, No. 3
69484/3666144
Mol Pharmacol 79:368–380, 2011
Printed in U.S.A.

A Serotype 5/3 Adenovirus Expressing MDA-7/IL-24 Infects Renal Carcinoma Cells and Promotes Toxicity of Agents That Increase Ros and Ceramide Levels

Margaret A. Park, Hossein A. Hamed, Clint Mitchell, Nichola Cruickshanks, Rupesh Dash, Jeremy Allegood, Igor P. Dmitriev, Gary Tye, Besim Ogretmen, Sarah Spiegel, Adly Yacoub, Steven Grant, David T. Curiel, Paul B. Fisher, and Paul Dent

Departments of Neurosurgery (M.A.P., C.M., H.A.H., N.C., G.T., A.Y., P.D.), Biochemistry and Molecular Biology (J.A., S.S.), Medicine (S.G.), and Human and Molecular Genetics (R.D., P.B.F.) and the VCU Institute of Molecular Medicine (R.D., S.G., P.B.F., P.D.), Virginia Commonwealth University, School of Medicine, Richmond, Virginia; Division of Human Gene Therapy, Departments of Medicine, Pathology, and Surgery, and the Gene Therapy Center, University of Alabama at Birmingham, Birmingham, Alabama (I.P.D., D.T.C.); and Department of Biochemistry and Molecular Biology, Medical University of South Carolina, Charleston, South Carolina (B.O.)

Received October 18, 2010; accepted November 30, 2010

ABSTRACT

Agents that generate reactive oxygen species (ROS) are recognized to enhance MDA-7/IL-24 lethality. The present studies focused on clarifying how such agents enhanced MDA-7/IL-24 toxicity in renal cell carcinoma cells (RCCs). Infection of RCCs with a tropism-modified serotype 5/3 adenovirus expressing MDA-7/IL-24 (Ad.5/3-*mda*-7) caused plasma membrane clustering of CD95 and CD95 association with pro-caspase 8, effects that were enhanced by combined exposure to 17-*N*-allylamino-17-demethoxygeldanamycin (17AAG), As_2O_3, or fenretinide and that correlated with enhanced cell killing. Knockdown of CD95 or expression of cellular FADD (Fas-associated protein with death domain)-like interleukin-1β–converting enzyme inhibitory protein, short form (c-FLIP-s) blocked enhanced killing. Inhibition of ROS generation, elevated cytosolic Ca^{2+}, or de novo ceramide synthesis blocked Ad.5/3-*mda*-7 $\pm$ agent-induced CD95 activation and the enhancement of apoptosis. Ad.5/3-*mda*-7 increased ceramide levels in a PERK-dependent fashion that were responsible for elevated cytosolic Ca^{2+} levels that promoted ROS generation; 17AAG did not further enhance cytokine-induced ceramide generation. In vivo, infection of RCC tumors with Ad.5/3-*mda*-7 suppressed the growth of infected tumors that was enhanced by exposure to 17AAG. Our data indicate that in RCCs, Ad.5/3-*mda*-7-induced ceramide generation plays a central role in tumor cell killing and inhibition of multiple signaling pathways may have utility in promoting MDA-7/IL-24 lethality in renal cancer.

This work was supported by the National Institutes of Health National Institute of Diabetes and Digestive and Kidney Diseases [Grant R01-DK52825] (to P.D.); the National Institutes of Health National Cancer Institute [Grants R01-CA108325, R01-CA141703, R01-CA150214] (to P.D.), [Grants R01-CA63753, R01-CA77141] (to S.G.), [Grants R01-CA097318, R01-CA127641, R01-CA134721] (to P.B.F.), and [Grant P01-CA104177] (to P.D., P.B.F., D.C., I.P.D.); The Jim Valvano "V" foundation (to P.D.); Department of Defense [Award DAMD17-03-1-0262] (to P.D.); the Leukemia Society of America [Grant 6405-97] (to S.G.); the Samuel Waxman Cancer Research Foundation (to P.B.F.); and the National Foundation for Cancer Research (to P.B.F.). P.D. is The Universal Inc. Professor in Signal Transduction Research. P.B.F. holds the Thelma Newmeyer Corman Chair in Cancer Research in the VCU Massey Cancer Center.

Article, publication date, and citation information can be found at http://molpharm.aspetjournals.org.

doi:10.1124/mol.110.069484.

Introduction

In the United States, renal cell carcinoma (RCC) is diagnosed in ~51,000 patients each year. If the disease is detected at an early stage, during which a large portion or the entire kidney can be removed with the tumor, a high level of prolonged patient survival is noted (Gillett et al., 2005 and references therein). However, if the disease has spread beyond the capsule of the kidney into the adrenal gland or surrounding fascia with nodal involvement, the prognosis is poor, with rapid nadir. This occurs even under ideal circum-

ABBREVIATIONS: RCC, renal cell carcinoma; IL, interleukin; ER, endoplasmic reticulum; PERK, protein kinase R-like endoplasmic reticulum kinase; GST, glutathione transferase; ROS, reactive oxygen species; MAPK, mitogen activated protein kinase; CAR, coxsackie and adenovirus receptor; 17AAG, 17-*N*-allylamino-17-demethoxygeldanamycin; 4HPR, *N*-(4-hydroxyphenyl) retinamide (fenretinide); DMSO, dimethyl sulfoxide; PAGE, polyacrylamide gel electrophoresis; moi, multiplicity of infection; si, small interfering; TUNEL, terminal deoxynucleotidyl transferase dUTP nick-end labeling; FBS, fetal bovine serum; PBS, phosphate-buffered saline; DISC, death-inducing signaling complex; VHL, Von Hippel Lindau; LASS, longevity assurance gene; CMV, cytomegalovirus (empty vector); MDA-7, melanoma differentiation associated gene-7; 5/3, serotype 5/serotype 3 adenovirus; Ad, adenovirus.

stances, where the disease is still only locally advanced, essentially all of the tumor can be surgically removed, and the patients are maximally treated with palliative radiation and chemotherapy. In part, this resistance occurs because RCC is characterized as frequently being highly refractory to multiple established cytotoxic chemotherapy regimens (Gillett et al., 2005).

The *mda*-7 gene [renamed interleukin (IL)-24] was isolated from human melanoma cells induced to terminally differentiate by treatment with interferon β and mezerein (Jiang et al., 1995). The protein expression of MDA-7/IL-24 is decreased during melanoma progression, with nearly imperceptible levels in metastatic disease (Jiang et al., 1995; Ekmekcioglu et al., 2001; Ellerhorst et al., 2002). Based on an internal amino acid signature motif, MDA-7/IL-24 was classified as a member of the IL-10 gene family (Huang et al., 2001; Caudell et al., 2002; Parrish-Novak et al., 2002; Fisher et al., 2003; Pestka et al., 2004; Fisher, 2005; Lebedeva et al., 2005; Gupta et al., 2006). Enforced expression of MDA-7/IL-24, by use of the recombinant adenovirus Ad.5-*mda*-7, inhibits the growth and kills a broad spectrum of cancer cells without exerting toxic effects in a wide assortment of nontransformed "normal" cell types (Su et al., 1998, 2001; Fisher et al., 2003; Fisher, 2005; Lebedeva et al., 2005; Gupta et al., 2006). *Mda*-7/IL-24 was evaluated in a phase I clinical trial in heavily pretreated patients with advanced cancers; in this study Ad.5-*mda*-7 (INGN-241) injected intratumorally was safe and, with repeated injections, resulted in significant clinical activity in many patients (Fisher et al., 2003; Cunningham et al., 2005; Lebedeva et al., 2005, 2007a).

The apoptotic pathways by which MDA-7/IL-24 kills tumor cells are still not fully understood; however, current evidence suggests an inherently high degree of complexity and an involvement of proteins important for the onset of growth inhibition and apoptosis, including BCL-XL, BCL-2, and BAX (Su et al., 1998, 2001; Lebedeva et al., 2002; Fisher, 2005; Gupta et al., 2006a; Park et al., 2009; Eulitt et al., 2010). In prostate cancer cells, overexpression of either BCL-2 or BCL-XL protects cells from MDA-7/IL-24 -induced toxicity in a cell type-dependent fashion (Su et al., 2006). In ovarian cancer, MDA-7/IL24 was reported to kill via the extrinsic apoptosis pathway (Gopalan et al., 2005), and we recently demonstrated that bacterially synthesized GST-MDA-7 killed multiple renal carcinoma cell lines, also via activation of CD95/FAS receptor (Park et al., 2009).

MDA-7/IL-24 toxicity has also been linked to alterations in endoplasmic reticulum (ER) stress signaling (Sarkar et al., 2002; Gupta et al., 2006a; Yacoub et al., 2008a,b). In these studies, MDA-7/IL-24 physically associates with BiP/GRP78 and inactivates the protective actions of this ER-chaperone protein as assessed by increased PKR-like endoplasmic reticulum kinase (PERK) autophosphorylation and increased phosphorylation of the downstream PERK target eukaryotic translation initiation factor 2α. In addition to virus-administered *mda*-7/IL-24, delivery of this cytokine as a bacterially expressed GST fusion protein, GST-MDA-7, retains cancer-specific killing and selective ER localization, and it induces similar signal transduction changes in cancer cells (Sauane et al., 2004a; Gupta et al., 2006a, 2008; Yacoub et al., 2008b, 2010). We have noted that high concentrations of GST-MDA-7 or infection with a serotype 5 virus, Ad.5-*mda*-7, to deliver the *mda*-7 transgene kills primary human glioma cells and does so in a PERK- and ceramide-dependent fashion that requires mitochondrial dysfunction but not activation of the extrinsic pathway (Yacoub et al., 2008b, 2010). Similar data were obtained in prostate cancer, a genitourinary malignancy. Thus, MDA-7/IL-24 lethality seems to occur by multiple distinct pathways in different tumor cell types, but in all of these studies, cell killing is reflected in a profound induction, downstream of primary effector molecules, in mitochondrial dysfunction.

Prior work with MDA-7/IL-24 in renal carcinoma cells and malignant gliomas, using bacterially synthesized GST-MDA-7 protein, demonstrated that in the low 0.25 to 2.0 nM concentration range, GST-MDA-7 primarily causes growth arrest with little cell killing, whereas at ~20-fold greater concentrations, this cytokine causes profound growth arrest and tumor cell death (Yacoub et al., 2003; Park et al., 2009). Agents that are known to promote the generation of reactive oxygen species (ROS) in tumor cells (e.g., As_2O_3 or 4-HPR) (Lebedeva et al., 2005a), promoted GST-MDA-7 toxicity that correlated with enhanced activation of p38 MAPK, signaling of which is a key proapoptotic signal caused by MDA-7/IL-24 expression (Sarkar et al., 2002). The precise mechanisms by which ROS-inducing agents interact with MDA-7/IL-24 to kill renal carcinoma cells (e.g., by altering MDA-7/IL-24–induced activation of CD95) are unknown.

In the clinic, MDA-7/IL-24 has been examined in a phase I study using a gene therapy approach by means of a recombinant serotype 5 adenovirus to deliver the *mda*-7/IL-24 gene (INGN-241) (Fisher et al., 2003; Cunningham et al., 2005; Fisher, 2005; Lebedeva et al., 2007a). Kidney cancer cells display low levels of the coxsackie and adenovirus receptor (CAR), resulting in many of the commercially available cell lines being relatively resistant to infection by a serotype 5 adenovirus. Using established human RCC lines, we have used a recently engineered novel chimeric serotype 5/serotype 3 adenovirus, Ad.5/3-*mda*-7, to deliver the *mda*-7/IL-24 gene to RCCs (Dash et al., 2010; Eulitt et al., 2010; Hamed et al., 2010). Using Ad.5/3-*mda*-7, we determined the molecular mechanisms upstream and proximal to CD95 activation by which MDA-7/IL-24 and agents that elevate ROS levels [17-*N*-allylamino-17-demethoxygeldanamycin (17AAG), As_2O_3, and fenretinide (4HPR)] interact to kill RCCs.

Materials and Methods

Materials

A plasmid expressing dominant-negative PERK was kindly supplied by Dr. A. Diehl (University of Pennsylvania, Philadelphia, PA). Commercially available validated short hairpin RNA molecules to knock down RNA/protein levels were from QIAGEN (Valencia, CA), as described elsewhere (Gupta et al., 2006a; Yacoub et al., 2008a,b, 2010; Park et al., 2010; Yacoub et al.). Antibody reagents, kinase and caspase inhibitors, cell culture reagents, and sources of noncommercial recombinant adenoviruses have been described previously (Gupta et al., 2006a; Yacoub et al., 2008a,b, 2010; Eulitt et al., 2010; Hamed et al., 2010; Park et al., 2010). Arsenic trioxide, 17AAG, and 4HPR were obtained from EMD Biosciences (Darmstadt, Germany).

Methods

Generation of Ad.5.mda-7 and Ad.5/3-mda-7. Recombinant serotype 5 and serotype 5/serotype 3 adenoviruses to express MDA-7/IL-24 ("Ad.*mda-7*"), control ("Ad.*cmv*" empty vector) were generated

in the laboratory of author D.T.C. as described elsewhere (Su et al., 1998; Dash et al., 2010; Hamed et al., 2010).

Synthesis of GST-MDA-7. GST and GST-MDA-7 were generated in bacteria and purified by glutathione affinity chromatography as described previously (Sauane et al., 2004a).

Cell Culture and In Vitro Exposure of cells To GST-MDA-7 and Drugs. All established RCC lines were cultured at 37°C [5% (v/v) CO_2] in vitro using RPMI 1640 medium supplemented with 5% (v/v) fetal calf serum and 10% (v/v) nonessential amino acids. The 786-0 lines transfected with empty vector or to express VHL were originally generated and supplied by Dr. W. Kaelin (Harvard University, Cambridge, MA). For short-term cell killing assays and immunoblotting, cells were plated at a density of 3×10^3 cells/cm^2; 24 h after plating, cells were treated with GST-MDA-7 or infected with Ad.5/3.*mda*-7 and/or various drugs, as indicated in the legend to each figure. In vitro small-molecule inhibitor treatments were from a 100 mM stock solution of each drug, and the maximal concentration of vehicle (DMSO) in media was 0.02% (v/v). Cells were not cultured in reduced serum media during any study.

Cell Treatments, SDS-PAGE, and Western Blot Analysis. Cells were treated with various GST-MDA-7 concentrations or infected with Ad.5/3-*mda*-7 at various multiplicities of infection (moi) as indicated in the figure legends. SDS-PAGE and immunoblotting was performed as described in the legend to each figure using standard techniques. In brief, at various time points after indicated treatment, hepatocytes were lysed in whole-cell lysis buffer (0.5 M Tris-HCl, pH 6.8, 2% SDS, 10% glycerol, 1% β-mercaptoethanol, and 0.02% bromphenol blue), and the samples were boiled for 30 min. The boiled samples were loaded onto 10 to 14% SDS-PAGE, and electrophoresis was run overnight. Proteins were electrophoretically transferred onto 0.22-μm nitrocellulose and immunoblotted with various primary antibodies against different proteins. All immunoblots were visualized using an Odyssey Infrared Imager (LI-COR Biosciences, Lincoln, NE) with associated software. For presentation, immunoblots were opened in PhotoShop CS2 (Adobe Systems, Mountain View, CA); the color was removed, and figures were generated in PowerPoint (Microsoft Corp., Redmond, WA) (Park et al., 2010).

Recombinant Adenoviral vectors; Infection In Vitro. We generated and purchased previously noted recombinant adenoviruses as described previously (Su et al., 1998; Gupta et al., 2006a; Yacoub et al., 2008a,b, 2010). Cells were infected with these adenoviruses at an appropriate moi as indicated in the figure legends. Cells were incubated for 24 h after infection to ensure adequate expression of transduced gene products before any subsequent drug exposures.

Detection of Cell Death by Trypan Blue, Hoechst, TUNEL, and Flow Cytometric Assays. Cells were harvested by trypsinization with Trypsin/EDTA for ~10 min at 37°C. As some apoptotic cells detached from the culture substratum into the medium, these cells were also collected by centrifugation of the medium at 1500 rpm for 5 min. The pooled cell pellets were resuspended. Trypan blue exclusion cell death assays were performed as individual assays in triplicate on each experimental occasion (Hamed et al., 2010; Yacoub et al., 2010).

Plasmid Transfection. Plasmid DNA (0.5 μg/total plasmid transfected) was diluted into 50 μl of RPMI 1640 growth media that lacked supplementation with FBS or with penicillin-streptomycin. Lipofectamine 2000 reagent (1 μl; Invitrogen, Carlsbad, CA) was diluted into 50 μl of growth media that lacked supplementation with FBS or with penicillin-streptomycin. The two solutions were then mixed together and incubated at room temperature for 30 min. The total mix was added to each well (4-well glass slide or 12-well plate) containing 200 μl of growth media that lacked supplementation with FBS or with penicillin-streptomycin. The cells were incubated for 4 h at 37°C, after which time the media was replaced with RPMI 1640 growth media containing 5% (v/v) FBS and 1× penicillin-streptomycin.

Mass Spectrometric Determination of Ceramide and Dihydroceramide Lipid Levels. A498 cells were scraped into PBS 6 h after exposure and isolated by centrifugation followed by freezing at −80°C. Lipids were isolated from the cells, and ceramide isoforms were analyzed by liquid chromatography and electrospray ionization-tandem mass spectrometry with a binary pump system (LC-10; Shimadzu, Columbia, MD) coupled to a PerkinElmer Series 200 autoinjector (PerkinElmer Life and Analytical Sciences, Waltham, MA) and a mass spectrometer (4000 Q TRAP; Applied Biosystems, Foster City, CA) operating in a triple quadrupole mode, as described previously (Hait et al., 2009).

Animal Studies. Athymic Nu/Nu mice (8 weeks old, female) were obtained from the NCI. Mice were irradiated (1.5 Gy) 48 h before injection of animals with 10^7 A498 cells further suppressing animal immune systems, thereby improving take rate. Tumors of ~150 mm^3 grew over the subsequent 29 days. Animals were segregated into tumor volumes of approximate equivalent mean tumor size and standard errors were determined. For studies in Fig. 6A, the tumor was injected with 2 μl (10^8 infectious particles) of either Ad.5/3-*cmv* or Ad.5/3-*mda*-7 suspended in 2 μl of PBS delivered by slow infusion over a 6-min period. Two days after the first virus infection, tumors were again infected in an identical fashion with adenovirus. The mean volumes of the tumors on each flank are presented as fold increase over the preinfected volume (defined as 1.00) ($n = 3$, ± S.E.M.; 9–10 mice per group total). For the studies in Fig. 6, B and C, adenoviral vector Ad.5/3-*mda*-7 or Ad.5/3-*cmv* was administered 29 days after tumor cell implantation into animals. Viral vector (Ad.5/3-*mda*-7 or Ad.*cmv*; 0.5×10^7 plaque-forming units) suspended in 2 μl of PBS was delivered by slow infusion over a 6-min period. This infection procedure was repeated 1 week later. Animals were treated 24 h after each virus infection with either vehicle, 4HPR (100 mg/kg), or 17AAG (10 mg/kg) every day for 3 days. Animals then received a 2-day treatment break. Tumor volumes were measured every 2 or 3 days, as indicated in the figure legends.

Immunohistochemistry and Staining of Fixed Tumor Sections. After sacrifice, tumors were fixed in Tissue-Tek O.C.T. compound (Sakura Finetek Europe, Zoeterwoude, the Netherlands) and cut into 12-μm sections on a cryostat (Leica, Wetzlar, Germany). Nonspecific binding was blocked with a 2% (v/v) rat sera, 1% (v/v) bovine sera, 0.1% (v/v) Triton X-100, and 0.05% (v/v) Tween 20 solution. Sections were then stained for apoptosis and growth markers: cleaved caspase 3 (rabbit IgG, 1:100; Cell Signaling Technology, Danvers, MA) and Ki67 (mouse IgG, 1:100; Santa Cruz Biotechnology, Santa Cruz, CA). For staining of sectioned tumors, primary antibodies were applied overnight, sections were washed with phosphate buffer solution, and fluorescein-tagged secondary antibodies were applied for detection (as indicated in Fig. 6C): goat antirat Alexa 488/647 (1:500; Invitrogen); goat anti-mouse Alexa 488/647 (1:500; Invitrogen); secondary antibody was selected per the primary antibody used. Sections were then dehydrated, cleared, and mounted with coverslips using 4,6-diamidino-2-phenylindole mounting media (Vector Laboratories, Burlingame, CA). Apoptotic cells with double-stranded DNA breaks were detected using a TUNEL apoptotic detection kit (Millipore, Billerica, MA) according to the manufacturer's instructions. Slides were applied to high-powered light/confocal microscopes (LSM 510 meta-confocal scanning microscope; HBO 100 microscope with Axio Cam MRm camera; Carl Zeiss GmbH, Jena, Germany). The proliferation zone, which included both tumor and normal tissue, was usually selected as the site of interest, within 2 mm of or juxtaposed to leading edge of the tumor.

Analysis of DISC Formation. Cells were lysed as described by Park et al. (2009, 2010)). Portions of lysate (5%) were used to determine total protein levels. The remaining portion of lysate was subjected to immunoprecipitation for CD95. The amount of coimmunoprecipitating caspase 8 was determined after SDS PAGE and anti-caspase 8 blotting.

Analysis of ROS and Cytosolic Ca^{2+} Levels. ROS levels were determined in a Vector 3 plate reader (PerkinElmer Life and Ana-

lytical Sciences) as described previously (Park et al., 2009; Yacoub et al., 2010). In brief, cancer cells were plated in 96-well plates. 2,7-Dichlorodihydro-fluorescein diacetate, which is nonfluorescent in its dihydro form but becomes highly fluorescent upon reaction with ROS to 2,7-dichlorofluorescin, was used to monitor production of cellular ROS. Cells were preincubated with dichlorodihydro-fluorescein diacetate (5 mmol/dm^3 for 30 min; Invitrogen). Fluorescence measurements were obtained 0 to 30 min after drug addition with a Vector 3 plate reader. Data are presented corrected for basal fluorescence of vehicle-treated cells at each time point and expressed as a fold increase in ROS levels. For cytosolic Ca^{2+} levels, carcinoma cells were seeded in 96-well plates with fura-2 acetoxymethyl ester as an indicator. The ratio of fura-2 acetoxymethyl ester emissions, when excited at wavelengths of 340 and 380 nm, was recorded, and analysis software supplied with the plate reader was used to process and statistically analyze data.

Data Analysis. Comparison of the effects of various treatments was performed using one-way analysis of variance and a two-tailed Student's *t* test. Differences with a p value of < 0.05 were considered statistically significant. Statistical examination of in vivo animal survival data used log rank statistical analyses between the different treatment groups. Experiments shown are the means of multiple individual independent points (at least three per experiment) from multiple experiments (at least two experiments; minimum independent points per value = 6) (± S.E.M.).

Results

MDA-7 Interacts with ROS-Producing Agents in a Greater-than-Additive fashion to Cause RCC Death; Killing Is Suppressed By Re-Expression of VHL. Initial experiments focused on defining the impact of GST-MDA-7 in combination with agents that generate intracellular ROS. In UOK121LN and A498 renal carcinoma cells, the lethality of GST-MDA-7 was enhanced in a greater-than-additive fashion by As_2O_3, 17AAG, and 4HPR (Fig. 1, A–C). The majority of RCCs in patients have lost expression of the Von Hippel Lindau (VHL) protein, an E3 ligase, resulting in an increased protein stress load in tumor cells (Turcotte et al., 2008). Re-expression of the VHL protein in 786-0 RCCs suppressed GST-MDA-7 toxicity and the interaction between GST-MDA-7 and 17AAG or As_2O_3 (Fig. 1D).

To achieve metastatic spread from the primary tumor site through the blood, tumor cells need to acquire some degree of resistance to undergoing anoikis-induced apoptosis. We generated anoikis-resistant A498 cells and determined the impact of this survival process on GST-MDA-7 lethality. Anoikis-resistant kidney cancer cells were more sensitive to MDA-7/IL-24 lethality than tumor cells that grow attached to a substratum (Fig. 1, E and F). Killing of anoikis and parental cells was blocked by inhibition of caspase 8.

Ad.5/3-*mda*-7 Infects and Kills Renal Carcinoma Cells and Secretes MDA-7 into the Growth Media, Where It Has a Toxic Bystander Effect on Uninfected RCCs. RCCs are resistant to infection by serotype 5 adenoviruses (e.g., Ad.5-*mda*-7) because they do not express the CAR (Yacoub et al., 2003). To circumvent this problem, we developed a chimeric serotype 5/serotype 3 modified knob-serotype adenovirus to deliver *mda*-7/IL-24 to RCCs: Ad.5/3-*mda*-7 (Dash et al., 2010; Eulitt et al., 2010; Hamed et al., 2010). Infection of primary renal epithelial cells that express CARs with Ad.5-*mda*-7 produced expression of MDA-7/IL-24 without causing significant toxicity to these nontransformed cells (Eulitt et al., 2010; data not shown). Infection of RCCs with Ad.5/3-*mda*-7 caused cell death, and this toxicity was enhanced in a greater-than-additive fashion by As_2O_3, 17AAG, and 4HPR (Fig. 2, A–C). Prior studies have shown that bacterially synthesized GST-MDA-7 kills RCCs by activating the death receptor CD95/FAS- receptor (Park et al., 2009).

MDA-7/IL-24 is a secreted cytokine, and we next determined whether direct infection of RCCs with Ad.5/3-*mda*-7 (which contains the *mda*-7 cDNA to express a nontagged form of the protein that in mammalian cells is glycosylated and also a dimer) permitted MDA-7/IL-24 to be secreted from an infected cell into the culture media, whether this secreted MDA-7/IL-24 could then act to kill uninfected RCCs, and by what mechanism this killed uninfected RCCs. Transfer of media containing MDA-7/IL-24 onto uninfected RCCs promoted cell killing, and the transfer of conditioned media containing the cytokine enhanced 17AAG and As_2O_3 toxicity in a CD95- and MDA-7/IL-24–dependent fashion within the cell treated with conditioned media (Fig. 2D). Data similar to those in Fig. 2D were obtained when nontransformed primary human renal epithelial cells were infected with Ad.5/3-*mda*-7 and conditioned media containing MDA-7/IL-24 transferred onto uninfected kidney cancer cells, resulting in tumor cell apoptosis (Fig. 2, E and F). A mutant form of MDA-7/IL-24 that lacked the secretion peptide signal did not display a bystander effect (data not shown) (Sauane et al., 2004a,b, 2008, 2010; Eulitt et al., 2010).

As_2O_3 and 17AAG Enhance Ad.5/3-*mda*-7–Induced Activation of CD95 in an ROS-Dependent Manner. As MDA-7/IL-24, regardless of synthetic origin or in combination with ROS-inducing agents, was killing RCCs via increased CD95/caspase 8 signaling, we determined whether these ROS-inducing agents were truly altering the levels of CD95 activation. Treatment of Ad.5/3-*mda*-7-infected cells with 17AAG or As_2O_3 enhanced CD95 surface localization and promoted caspase 8 association with CD95 (DISC formation) (Fig. 3A). Similar data were obtained with 4HPR (data not shown). In agreement with prior studies and data in Figs. 1E and 2D showing death receptor dependence for cell killing, overexpression of the caspase 8 inhibitor c-FLIP-s blocked the enhancement of Ad.5/3-*mda*-7 lethality by 17AAG (Fig. 3B) (Park et al., 2009). Ad.5/3-*mda*-7 and 17AAG or 4HPR interacted to cause a dramatic greater-than-additive increase in the levels of ROS in RCCs, an effect that was blocked by overexpression of thioredoxin, by quenching of cytosolic Ca^{2+} using calbindin, by knockdown of ceramide synthase 6 (LASS6) expression, or by expression of dominant-negative PERK (Fig. 3, C and D, data not shown). It is noteworthy that although thioredoxin reduced As_2O_3-induced ROS production, neither calbindin nor knockdown of LASS6 expression, in contract to data using 17AAG or 4HPR, suppressed the As_2O_3-induced ROS levels. (Fig. 3D).

Ad.5/3-*mda*-7 Increases CD95 Surface Levels, An Effect That Is Enhanced by 17AAG or As_2O_3 and Blocked by Quenching of ROS or Ca^{2+} or Inhibition of De Novo Ceramide Synthesis. The increase in cell surface CD95 levels caused by Ad.5/3-*mda*-7 and 17AAG treatment was blocked by the quenching of ROS, the quenching of Ca^{2+}, or knockdown of LASS6 (Table 1). Quenching of ROS using thioredoxin also suppressed enhanced levels of induced CD95 tyrosine phosphorylation, DISC formation, and the ability of 17AAG and As_2O_3 to kill RCCs (Fig. 3, E and F).

17AAG and Fenretinide Enhance Ad.5/3-*mda*-7–Induced Cytosolic Ca^{2+} Levels, an Effect Blocked by Molecular Quenching of De Novo Ceramide Synthesis and By Expression of Dominant-Negative PERK; As_2O_3-Induced Cytosolic Ca^{2+} Levels are ROS-Dependent. Treatment of Ad.5/3-*mda*-7-infected cells with As_2O_3, 17AAG, or 4HPR enhanced cytosolic Ca^{2+} levels (Fig. 4A). It is noteworthy that quenching of ROS blocked neither 17AAG- nor 4HPR-induced Ca^{2+} levels, whereas quenching of ROS blocked As_2O_3-induced Ca^{2+} levels. Quenching of Ca^{2+} significantly reduced the increase in CD95 plasma membrane levels and reduced DISC formation (Table 1 and Fig. 4B). Quenching of Ca^{2+} also suppressed the ability of As_2O_3, 17AAG, or 4HPR to kill RCCs (Fig. 4C, data not shown). Based on these findings, and our prior analyses in glioblastoma and prostate cancer cells showing that MDA-7/IL-24 expression can lead to increased ceramide levels, we determined whether ceramide generation was involved in the interaction between Ad.5/3-*mda*-7 and As_2O_3/17AAG/4HPR (Park et al., 2009; Sauane et al., 2010).

Ad.5/3-*mda*-7–Induced CD95 Activation Is Dependent on the De Novo Ceramide Synthesis Pathway. Ad.5/3-*mda*-7-induced CD95 plasma membrane localization

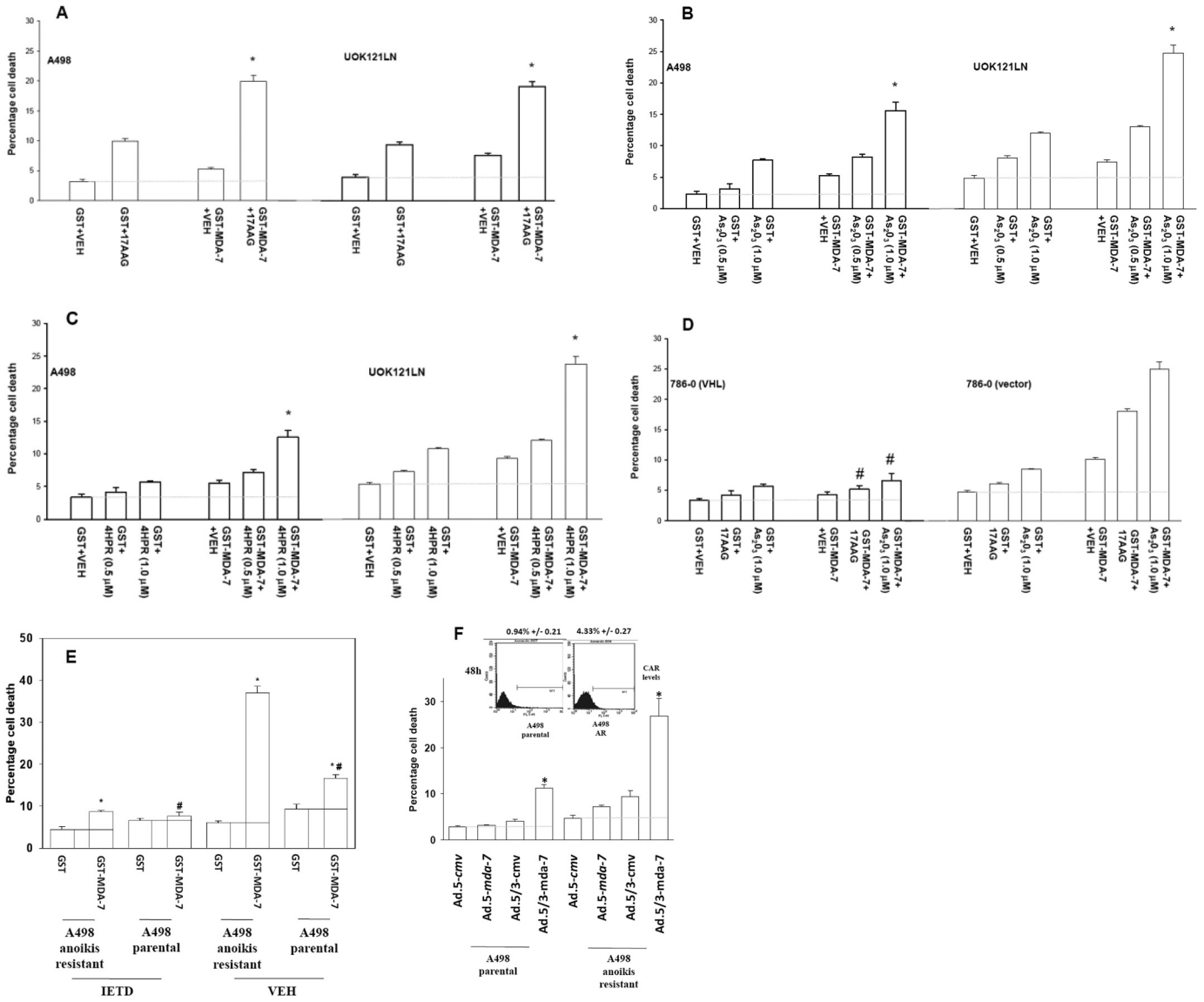

Fig. 1. GST-MDA-7 interacts with ROS-producing agents in a greater-than-additive fashion to cause RCC death; killing is suppressed by re-expression of VHL. A to C, UOK121LN and A498 cells were treated 24 h after plating with GST or GST-MDA-7 (1 nM) and in parallel with vehicle (DMSO) and either 17AAG (100 nM), As_2O_3 (0.5, 1.0 μM), or 4HPR (0.5, 1.0 μM). Forty-eight hours after GST-MDA-7 treatment, cell viability was determined using trypan blue exclusion ($n = 3$, $\pm$ S.E.M.; $*$, $p < 0.05$ greater than corresponding treatment with GST). D, parental VHL-null 786-0 cells transfected with empty vector or 786-0 cells stably transfected to express VHL were treated 24 h after plating with GST or GST-MDA-7 (1 nM) and in parallel with either vehicle (DMSO), 17AAG (100 nM), or As_2O_3 (0.5 and 1.0 μM). Forty-eight hours after GST-MDA-7 treatment, cell viability was determined using trypan blue dye exclusion ($n = 3$, $\pm$ S.E.M.; #, $p < 0.05$ less than corresponding values in with vector cells). E, A498 cells (parental and anoikis-resistant) were treated with GST or GST-MDA-7 (20 nM) in the presence or absence of vehicle (DMSO) or the caspase 8 inhibitor IETD (50 μM). Cell viability was determined by trypan blue dye exclusion assay after 48 h ($n = 3$, $\pm$ S.E.M.; $*$, $p < 0.05$ greater than corresponding treatment with GST; #, $p < 0.05$ less than corresponding value in anoikis-resistant cells). F, A498 cells (parental and anoikis-resistant) were infected with Ad.5-*cmv*, Ad.5/3-*cmv*, Ad.5-*mda*-7, or Ad.5/3-*mda*-7 (20 moi), and 48 h later, viability was determined by trypan blue dye exclusion assay ($n = 3$, $\pm$ S.E.M.). Top inset, the levels of cell surface CAR were determined using an anti-CAR antibody labeled with FITC via flow cytometry ($n = 3$, $\pm$ S.E.M.; $*$, $p < 0.05$ greater than corresponding treatment with Ad.5/3-*cmv*).

was blocked by inhibition of the de novo ceramide synthesis pathway (Table 1 and Fig. 5A, lower graph). The abilities of 4HPR, 17AAG, and As_2O_3 to stimulate CD95 surface localization and DISC formation were also blocked by inhibition of the de novo ceramide synthesis pathway (Table 1 and Fig. 5, A, lower graph and upper blot). Ad.5/3-*mda*-7–induced tumor

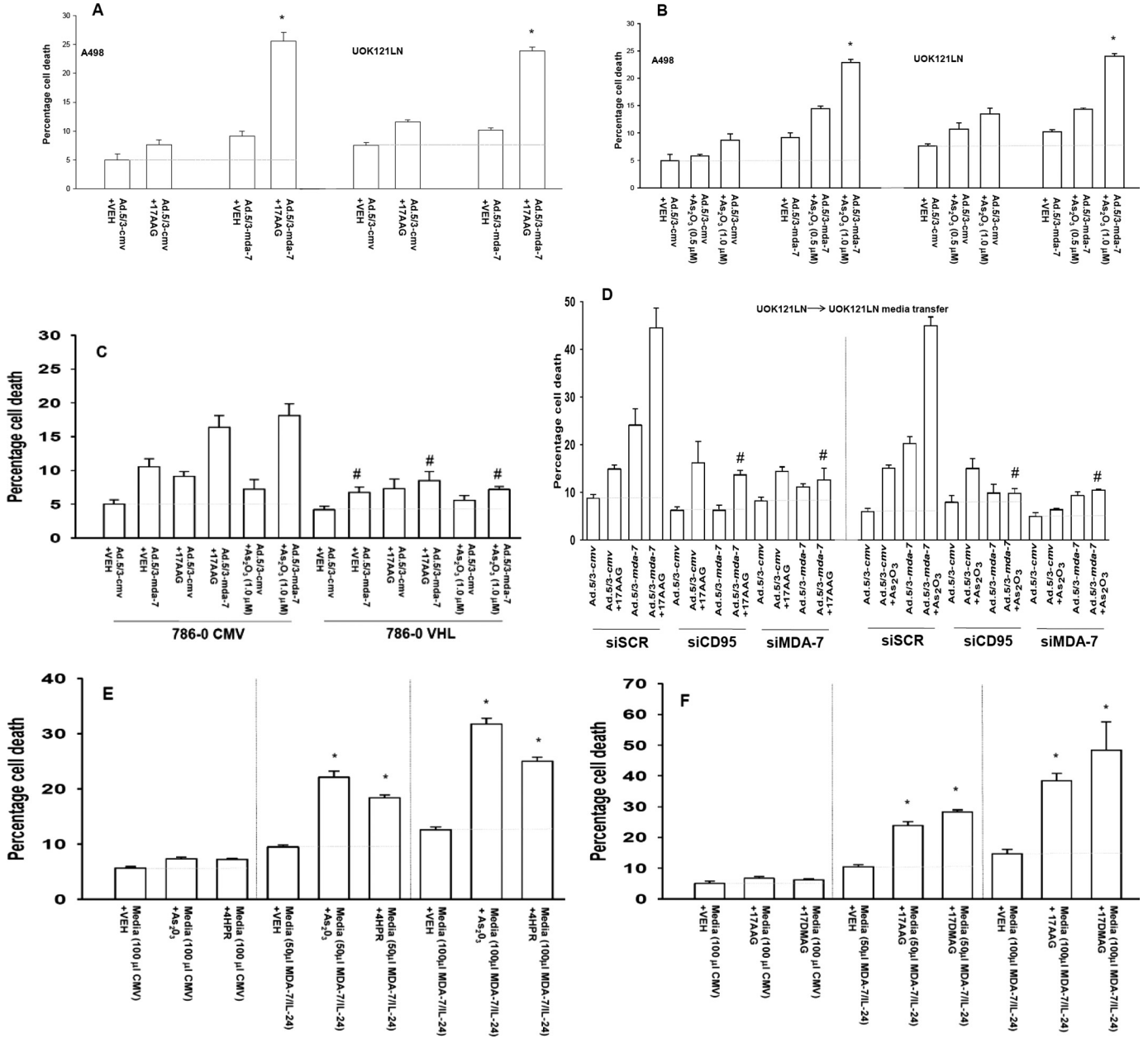

Fig. 2. A serotype 5/serotype 3 recombinant adenovirus to express MDA-7/IL-24 (Ad.5/3-*mda*-7) infects and kills renal carcinoma cells. A and B, UOK121LN and A498 cells were infected 24 h after plating with Ad.5/3-*cmv*, Ad.5/3-*mda*-7 (20 moi), and 12 h after infection treated with vehicle (DMSO) or either 17AAG (100 nM) or As_2O_3 (0.5 and 1.0 μM). Forty-eight hours after infection, cell viability was determined using trypan blue dye exclusion ($n = 3$, $\pm$ S.E.M.; $*$, $p < 0.05$ greater than corresponding treatment with Ad.5/3-*cmv*). C, parental VHL-null 786-0 cells transfected with empty vector or 786-0 cells stably transfected to express VHL were infected 24 h after plating with Ad.5/3-*cmv* or Ad.5/3-*mda*-7 (20 moi) and 12 h after infection treated with vehicle (DMSO) or either 17AAG (100 nM) or As_2O_3 (0.5, 1.0 μM). Forty-eight hours after infection, cell viability was determined using trypan blue dye exclusion ($n = 3$, $\pm$ S.E.M.; #, $p < 0.05$ less than corresponding treatment in CMV vector cells). D, UOK121LN cells were transfected with either scrambled siRNA molecules (siSCR) or molecules to knock down expression of CD95 (siCD95) or MDA-7/IL-24 (siMDA-7), as indicated. In parallel, other portions of UOK121LN cells were infected with Ad.5/3-*cmv* or Ad.5/3-*mda*-7 (50 moi), and the growth media were isolated 48 h after infection. Transfected UOK121LN cells were treated with conditioned media in parallel with vehicle (DMSO), 17AAG (100 nM) or As_2O_3 (0.5 μM). Cell viability in the transfected cells was determined 48 h after treatment by trypan blue exclusion ($n = 3$, $\pm$ S.E.M.; #, $p < 0.05$ less than corresponding treatment with in siSCR cells). E, conditioned media from infected primary renal epithelial cells was placed onto UOK121LN cells, and cells were treated in parallel with vehicle (DMSO), 4HPR (0.5 μM), or As_2O_3 (0.5 μM). Cells were isolated 48 h after treatment with conditioned media, and viability was determined by trypan blue exclusion ($n = 3$, $\pm$ S.E.M.; $*$, $p < 0.05$ greater than corresponding treatment with media from Ad.5/3-*cmv* infected cells). F, conditioned media from infected primary renal epithelial cells were placed onto UOK121LN cells, and cells were treated in parallel with either vehicle (DMSO), 17AAG (0.1 μM), or 17-demethoxy-17-[[2-(dimethylamino)ethyl]amino]geldanamycin hydrochloride (0.1 μM). Cells were isolated 48 h after treatment with conditioned media and viability was determined by trypan blue dye exclusion ($n = 3$, $\pm$ S.E.M.; $*$, $p < 0.05$ greater than corresponding treatment with media from Ad.5/3-*cmv* infected cells).

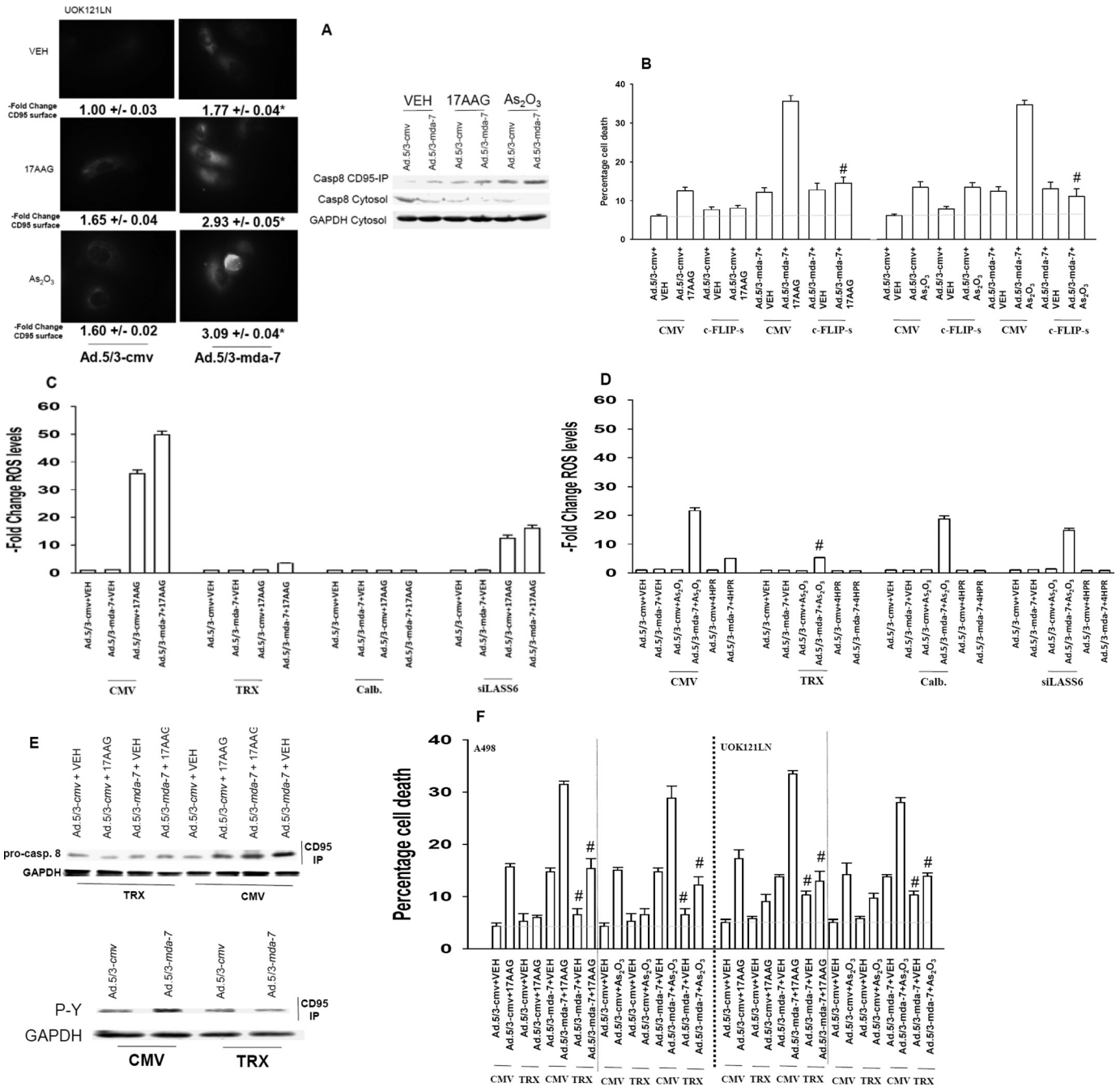

Fig. 3. As_2O_3 and 17AAG enhance Ad.5/3-*mda*-7–induced activation of CD95 in an ROS-dependent manner. A, UOK121LN cells, in four-well chambered slides or 60-mm dishes, were infected with Ad.5/3-*cmv* or Ad.5/3-*mda*-7 (50 moi). Twenty-four hours after infection, cells were treated with vehicle (DMSO), 17AAG (100 nM), or As_2O_3 (0.5 μM); 6 h later, cells were fixed for determination of CD95 plasma membrane levels or were lysed for immunoprecipitation of CD95 for determination of caspase 8-CD95 association (DISC complex formation). Immunohistochemistry data from 40 cells per experiment ($n = 3$, $\pm$ S.E.M.; $*$, $p < 0.05$ greater than corresponding treatment with media from Ad.5/3-*cmv*–infected cells). DISC immunoblotting data, on the right, is from a representative of three independent studies. B, UOK121LN cells were transfected with either empty-vector control plasmid (CMV) or a plasmid to express c-FLIP-s. Twelve hours after transfection, cells were infected with Ad.5/3-*cmv* or Ad.5/3-*mda*-7 (50 moi). Twenty-four hours after infection cells were treated with vehicle (DMSO), 17AAG (100 nM), or As_2O_3 (0.5 μM). Forty-eight hours after infection, cells were isolated, and viability was determined by trypan blue dye exclusion assay ($n = 3$, $\pm$ S.E.M.; #, $p < 0.05$ less than corresponding treatment in CMV vector cells). C and D, UOK121LN cells in sextuplicate were transfected with empty-vector plasmid (CMV) and plasmids to express thioredoxin (TRX), calbindin D28 (Calb.), or to knockdown ceramide synthase 6 expression (siLASS6). Twelve hours after transfection, cells were infected with Ad.5/3-*cmv* or Ad.5/3-*mda*-7 (50 moi). Twenty-four hours after infection, cells were loaded with dichloro-dihydrofluorescein and then treated with vehicle (DMSO) or with 4HPR (0.5 μM), As_2O_3 (0.5 μM), or 17AAG (100 nM). The levels of ROS in cells were examined 1 h (17AAG and As_2O_3) or 2 h (4HPR) after drug addition ($n = 2$, 12 data points, $\pm$ S.E.M.; #, $p < 0.05$ less than corresponding treatment in CMV vector cells). E, UOK121LN cells were transfected with either empty-vector control plasmid (CMV) or a plasmid to express thioredoxin (TRX). Twelve hours after transfection, cells were infected with Ad.5/3-*cmv* or Ad.5/3-*mda*-7 (50 moi). Twenty-four hours after infection, cells were treated with vehicle (DMSO), 17AAG (100 nM), or As_2O_3 (0.5 μM). Six hours after drug treatment, cells were isolated and CD95 was immunoprecipitated to determine caspase 8 association and CD95 tyrosine phosphorylation. Representative studies are shown ($n = 3$). F, UOK121LN and A498 cells were transfected with either empty-vector control plasmid (CMV) or a plasmid to express thioredoxin (TRX). Twelve hours after transfection, cells were infected with Ad.5/3-*cmv* or Ad.5/3-*mda*-7 (50 moi). Twenty-four hours after infection, cells were treated with vehicle (DMSO), 17AAG (100 nM), or As_2O_3 (0.5 μM). Twenty-four hours after drug treatment, cells were isolated and viability determined by trypan blue dye exclusion assay ($n = 3$, $\pm$ S.E.M.; #, $p < 0.05$ less than corresponding treatment in CMV vector cells lacking thioredoxin).

cell killing and the abilities of 4HPR and 17AAG to further stimulate tumor cell death in the presence of MDA-7/IL-24 were also blocked by inhibition of the de novo ceramide synthesis pathway or knockdown of LASS6 expression (Fig. 5, B and C). Ad.5/3-*mda*-7 increased the levels of C16 ceramide and C16 dihydro-ceramide in RCCs in a PERK- and LASS6-dependent fashion (Fig. 5D, data not shown). Combined exposure of cells to Ad.5/3-*mda*-7 and to 17AAG did not further enhance ceramide generation; however, the combination of agents did permit ceramide generation when dominant-negative PERK was expressed.

Ad.5/3-*mda*-7 Infection of RCC Tumors Suppresses RCC Tumor Growth That Is Enhanced by 17AAG. Finally, because our medium-term aim is to translate MDA-7/IL-24 as a kidney cancer therapy into the clinic, we wished to determine whether MDA-7/IL-24 1) exhibited a bystander effect in vivo, 2) prolonged animal survival, and 3) could exhibit any interaction between 4HPR or 17AAG. To address the first issue, we established tumors on both flanks of an athymic mouse and injected one tumor with either an empty vector virus or a virus to express MDA-7/IL-24. Both the injected and noninjected contralateral tumor in Ad.5/3-*mda*-7-infected animals displayed a reduced growth rate that correlated with increased animal survival: 50% of the Ad.5/3-*cmv*–infected animals had to be sacrificed 10 days after virus infection compared with a 50% survival at 29 days after Ad.5/3-*mda*-7 infection (data not shown, $p < 0.05$ survival greater than Ad.5/3-*cmv*).

To determine whether MDA-7/IL-24 toxicity could be enhanced in vivo, we titrated downward and used 20-fold less Ad.5/3-*mda*-7 than in our prior studies (Eulitt et al., 2010; Hamed et al., 2010). A498 RCC tumors were established on one flank of an athymic mouse after ~29 days, the tumor was injected with Ad.5/3-*cmv* or with Ad.5/3-*mda*-7 (total of two injections), and animals were treated with 4HPR or 17AAG for the subsequent 3 days. Infection of tumors with a 20-fold lower dose of Ad.5/3-*mda*-7 did not significantly reduce the growth rate of tumors (Fig. 6, A and B). Surprisingly, on the basis of our in vitro interactions, 4HPR (fenretinide) did not significantly enhance Ad.5/3-*mda*-7 toxicity (at least at the dose and administration schedule tested herein), whereas 17AAG did further reduce tumor growth (Fig. 6, A and B) Reduced growth in Ad.5/3-*mda*-7 + 17AAG-treated tumors correlated with tumor cytoarchitecture disruption, decreased Ki67 staining, and increased caspase 3 cleavage and TUNEL staining (Fig. 6C).

Discussion

Previous studies from our laboratories have demonstrated that bacterial synthesized GST-MDA-7 reduces proliferation and causes tumor cell- and transformed cell-specific killing and radiosensitization in glioma and breast, prostate, and renal cancer cells. We noted that GST-MDA-7 killed RCCs by promoting activation of the death receptor CD95 and that single-agent killing also required ROS and ceramide production. The studies in this article were designed to determine the mechanisms by which clinically relevant agents that generate ROS promote mammalian cell synthesized MDA-7/IL-24 toxicity in RCCs.

RCCs are relatively resistant to infection by serotype 5 adenoviruses because of low CAR levels (e.g., Yacoub et al., 2003). Considering this problem in using serotype 5 adenoviruses for gene transduction in RCCs, we used a novel chimeric serotype 5/serotype 3 adenovirus, Ad.5/3-*mda*-7 (Dash et al., 2010; Eulitt et al., 2010; Hamed et al., 2010), that infects tumor cells using the CD46/80/86 receptors. The Ad.5/3-*mda*-7 virus readily infected multiple RCC cell lines with a subsequent robust expression of MDA-7/IL-24 protein. Overexpression of c-FLIP-s or the knockdown of CD95 expression reduced Ad.5/3-*mda*-7 toxicity in RCCs.

In our initial report examining MDA-7/IL-24 toxicity in RCCs, detailing the interactions between GST-MDA-7 and 4HPR/As_2O_3, we demonstrated that agents that generate ROS enhance MDA-7/IL-24 lethality (Yacoub et al., 2003). Similar combination effects between *mda*-7/IL-24 and ROS-inducing agents have also been observed in prostate and pancreatic cancer (Lebedeva et al., 2005a, 2007b). We subsequently noted that *unlike* GBM and prostate cancer cells, MDA-7/IL-24 (GST-MDA-7) killed RCCs by causing activation of the CD95 death receptor and activation of the extrinsic apoptosis pathway (Park et al., 2009). Our present findings have now determined the molecular mechanisms by which MDA-7/IL-24–induced cell killing is enhanced by ROS-inducing agents in RCCs, using glycosylated untagged dimeric MDA-7/IL-24, by employing a novel chime-

TABLE 1

Ad.5/3-*mda*-7 increases CD95 surface levels, an effect that is enhanced by 17AAG or As_2O_3 and blocked by quenching of ROS or Ca^{2+} or inhibition of de novo ceramide synthesis

UOK121LN cells in four-chambered glass slides were transfected with vector control plasmid (CMV or siSCR) or with plasmids to quench ROS (thioredoxin) or Ca^{2+} (calbindin D28) or to knock down ceramide synthase 6 expression (siLASS6). Twelve hours after transfection, cells are infected with Ad.5/3-*cmv* or Ad.5/3-*mda*-7. Twenty-four hours after infection, cells are treated with vehicle or MnTBAP (10 μM) as indicated and then with vehicle, 17AAG (100 nM), or As_2O_3 (0.5 μM). Cells were fixed 6 h after 17AAG/As_2O_3 treatment. Cell-surface levels of CD95 were determined by immunohistochemisty as described under *Materials and Methods*, with the cell-surface density of CD95 determined in 40 cells per experiment per condition ($n = 3$, ± S.E.M.).

Basal CD95 Surface Levels	Ad.5/3-*cmv*			Ad.5/3-*mda*-7		
	+ VEH	+ 17AAG	+ As_2O_3	+ VEH	+ 17AAG	+ As_2O_3
CMV + VEH	1.00 ± 0.06	1.79 ± 0.09	2.25 ± 0.11	3.58 ± 0.08*	6.50 ± 0.10*	5.21 ± 0.07*
CMV + MnTBAP	1.00 ± 0.04	1.52 ± 0.05	1.64 ± 0.09	2.25 ± 0.05†	3.32 ± 0.12†	2.22 ± 0.07†
TRX + VEH	1.00 ± 0.04	1.47 ± 0.05	1.35 ± 0.10	1.11 ± 0.03†	1.29 ± 0.06†	1.71 ± 0.07†
Calb +VEH	1.00 ± 0.05	1.50 ± 0.06	2.04 ± 0.09	2.06 ± 0.09†	2.16 ± 0.08†	2.29 ± 0.09†
siSCR + VEH	1.00 ± 0.08	1.71 ± 0.06	1.79 ± 0.06	2.60 ± 0.05*	3.20 ± 0.06*	3.26 ± 0.06*
siLASS6 + VEH	1.00 ± 0.03	1.07 ± 0.04	0.97 ± 0.03	1.16 ± 0.05†	0.97 ± 0.06†	1.31 ± 0.05†
siSCR + MYR	1.00 ± 0.07	1.27 ± 0.06	1.39 ± 0.04	1.37 ± 0.07†	1.40 ± 0.07†	1.97 ± 0.04†

siSCR, small interfering scrambled; TRX, thioredoxin; Calb, calbindin D28; MnTBAP, manganese(III) tetrakis(4-benzoic acid)porphyrin chloride; MYR, myriocin; VEH, vehicle.

* $P < 0.05$ greater than corresponding Ad.5/3-*cmv* infected value.

† $P < 0.05$ less than Ad.5/3-*mda*-7 + VEH value.

ric serotype modified adenovirus to deliver the *mda*-7/IL-24 transgene.

A priori we would have predicted that As_2O_3 would enhance MDA-7/IL-24 toxicity via its degeneration, causing additional generation of ROS and mitochondrial dysfunction, and not by causing further activation of CD95. 4HPR would kill by promoting additional ceramide generation that would increase MDA-7/IL-24–induced CD95 activation by increasing ceramide levels in lipid rafts. 17AAG would enhance MDA-7/IL-24 toxicity by causing additional generation of ROS and loss of protective signaling pathway activities and not by causing further activation of CD95. We determined that As_2O_3, 4HPR, and 17AAG all enhanced MDA-7/IL-24–induced activation of CD95 in RCCs, as judged by plasma membrane localization, increased CD95 tyrosine phosphorylation, and enhanced DISC formation/caspase 8 association. The enhanced amount of CD95 activation was dependent on the enhanced levels of ROS, Ca^{2+}, and ceramide generated in cells treated with Ad.5/3-*mda*-7 and with MDA-7/IL-24 combined with the agents 4HPR or 17AAG. In this regard, it is well known that 4HPR can increase ceramide levels in cells, and this effect has also been linked to the ability of this agent to elevate ROS production (Lai and Wong, 2008). The HSP90 antagonist 17AAG has been shown by our group and by others to increase ROS levels, in part based on the chemical structure of this drug but also potentially by inhibiting expression of ROS detoxification enzymes (Mitchell et al., 2007; Park et al., 2008; Azad et al., 2009). Nonetheless, without CD95 signaling, 17AAG was not effective at promoting MDA-7/IL-24 lethality.

We noted that 4HPR or 17AAG promoted Ad.5/3-*mda*-7–induced ROS and Ca^{2+} levels. For both 4HPR and 17AAG,

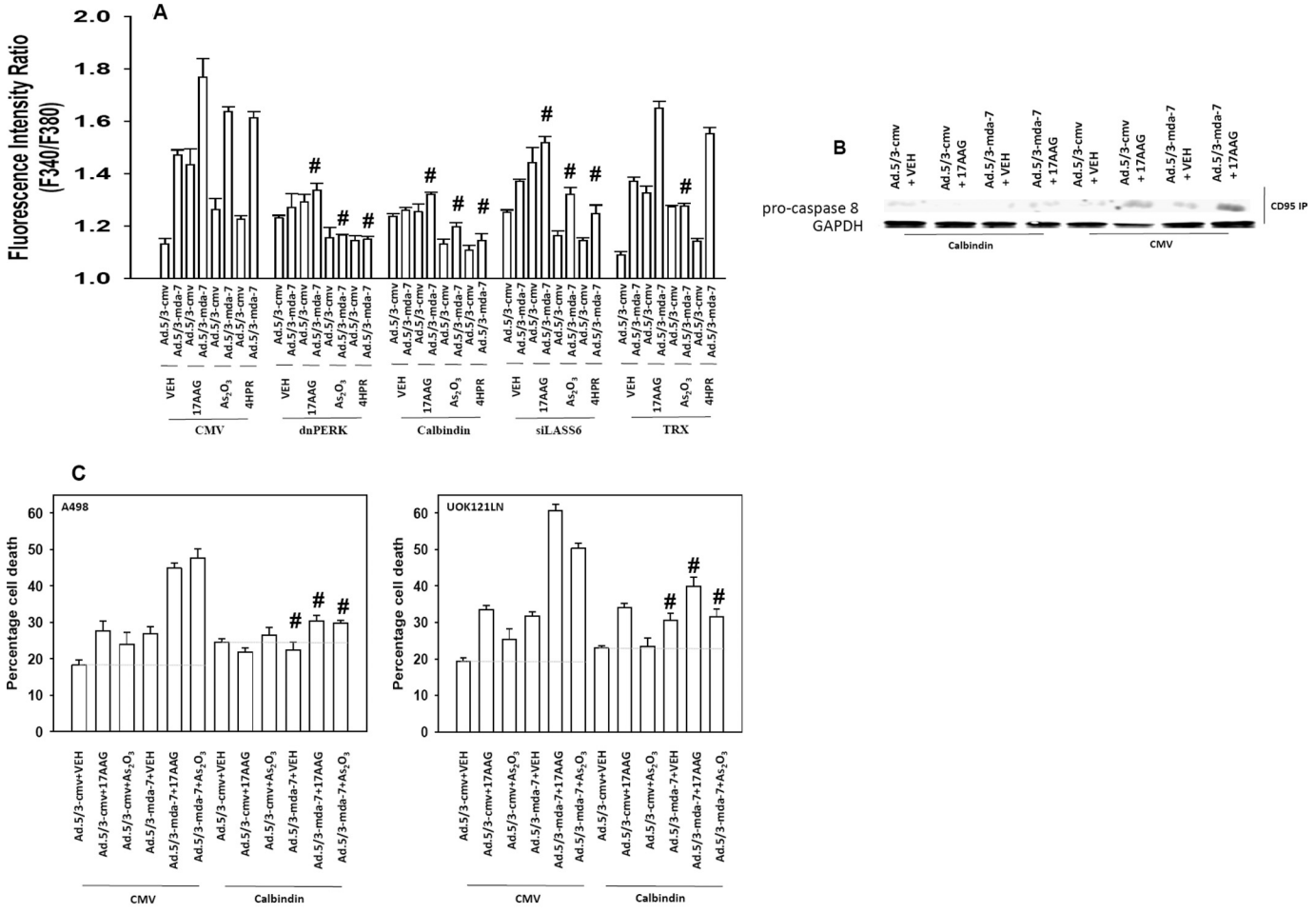

Fig. 4. 17AAG and 4-HPR enhance Ad.5/3-*mda*-7–induced Ca^{2+} levels, an effect blocked by molecular quenching of de novo ceramide synthesis and by expression of dominant-negative PERK; As_2O_3-induced Ca^{2+} levels are ROS-dependent. A, UOK121LN cells in sextuplicate were transfected with empty-vector plasmid (CMV) and plasmids to express dominant-negative PERK, thioredoxin (TRX), or calbindin D28 (Calb.) or to knock down ceramide synthase 6 expression (siLASS6). Twelve hours after transfection, cells were infected with Ad.5/3-*cmv* or Ad.5/3-*mda*-7 (50 moi). Twenty-four hours after infection, cells were loaded with Fura-2 and then treated with vehicle (DMSO), 4-HPR (0.5 μM), or 17AAG (100 nM). The levels of Ca^{2+} in cells were examined 1 h (17AAG) or 2 h (4HPR) after drug addition ($n = 2$, 12 data points, $\pm$ S.E.M.; #, $p < 0.05$ less than corresponding treatment in CMV vector cells). B, UOK121LN cells were transfected with empty-vector plasmid or a plasmid to express calbindin D28. Twelve hours after transfection, cells were infected with Ad.5/3-*cmv* or Ad.5/3-*mda*-7 (50 moi). Twenty-four hours after infection, cells were treated with vehicle (DMSO) or 17AAG (100 nM). Six hours after drug exposure, cells were isolated and CD95 immuno-precipitated. The amount of caspase 8 associated with CD95 was determined after PAGE/blotting ($n = 3$ independent studies). C, A498 and UOK121LN cells were transfected independently in triplicate with empty-vector plasmid or a plasmid to express calbindin D28. Twelve hours after transfection, cells were infected with Ad.5/3-*cmv* or Ad.5/3-*mda*-7 (50 moi). Twenty-four hours after infection, cells were treated with vehicle (DMSO) or 17AAG (100 nM). Cells were isolated 24 h after drug exposure, and viability was determined by trypan blue dye exclusion ($n = 2$, $\pm$ S.E.M.; #, $p < 0.05$ less than corresponding treatment in CMV vector cells).

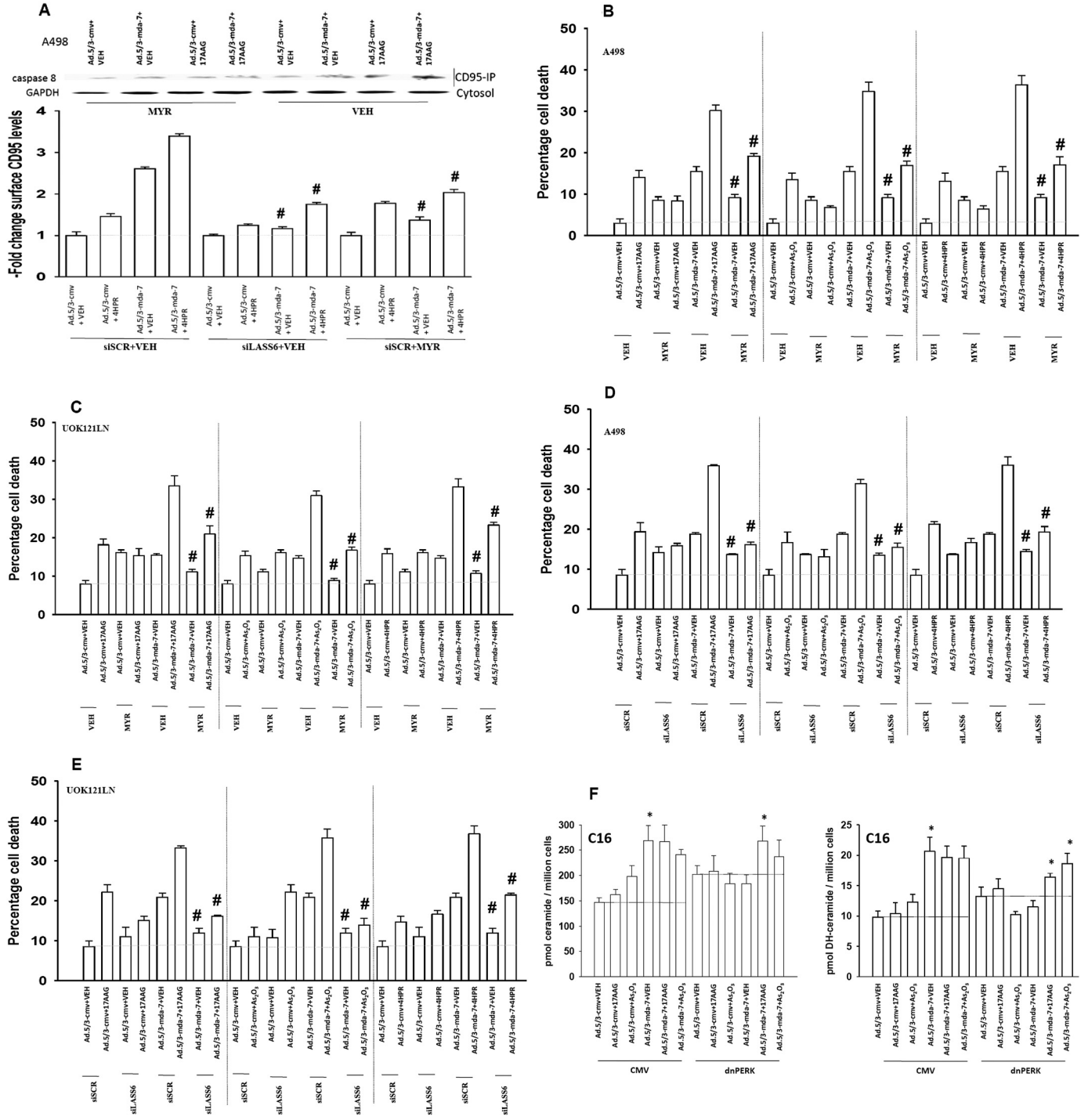

Fig. 5. Ad.5/3-*mda*-7–induced CD95 activation is dependent on the de novo ceramide synthesis pathway. A, A498 cells in four-well chambered slides or 60-mm dishes were transfected with empty-vector plasmid to express a scrambled siRNA or a plasmid to knockdown ceramide synthase 6 (siLASS6). Twelve hours after transfection cells were infected with Ad.5/3-*cmv* or Ad.5/3-*mda*-7 (50 moi) and treated with either vehicle (DMSO) or myriocin (1 μM). Twenty-four hours after infection, cells were treated with vehicle (DMSO), 4HPR (0.5 μM), or 17AAG (100 nM), as indicated. Six hours after drug exposure, cells were either fixed for immunohistochemistry to determine the levels of plasma membrane CD95 (lower graph) or lysed followed by CD95 immunoprecipitation to determine caspase 8 association (DISC) complex formation (upper immunoblot) ($n = 3$, $\pm$ S.E.M.; #, $p < 0.05$ less than corresponding treatment in siSCR cells). B and C, A498 and UOK121LN cells were infected independently in triplicate with Ad.5/3-*cmv* or Ad.5/3-*mda*-7 (50 moi) and treated with either vehicle (DMSO) or myriocin (1 μM). Twenty-four hours after infection, cells were treated as indicated with vehicle (DMSO), 4HPR (0.5 μM), or 17AAG (100 nM). Cells were isolated 24 h after drug-exposure and viability determined by trypan blue dye exclusion [$n = 2$, $\pm$ S.E.M.; # $p < 0.05$ less than corresponding treatment in vehicle-treated (VEH) cells]. D and E, A498 and UOK121LN cells were transfected independently in triplicate with empty-vector plasmid to express a scrambled siRNA or a plasmid to knockdown ceramide synthase 6 (siLASS6). Twelve hours after transfection, cells were infected with Ad.5/3-*cmv* or Ad.5/3-*mda*-7 (50 moi). Twenty-four hours after infection, cells are treated as indicated with vehicle (DMSO), 4HPR (0.5 μM), or 17AAG (100 nM). Cells were isolated 24 h after drug exposure, and viability was determined by trypan blue dye exclusion ($n = 2$, $\pm$ S.E.M.; #, $p < 0.05$ less than corresponding treatment in VEH cells). F, A498 cells were transfected independently in triplicate with empty-vector plasmid or a plasmid to express dominant-negative PERK. Twelve hours after transfection, cells were infected with Ad.5/3-*cmv* or Ad.5/3-*mda*-7 (50 moi). Twenty-four hours after infection, cells were treated as indicated with vehicle (DMSO) or 17AAG (100 nM). Cells were isolated 6 h after drug exposure, and the levels of ceramide determined by mass spectrometry ($n = 2$, $\pm$ S.E.M.; *, $p < 0.05$ greater than corresponding Ad.5/3-*cmv* control).

the enhanced generation of ROS was Ca^{2+}-dependent. Inhibition of the de novo ceramide synthesis pathway, or specifically knockdown of LASS6, suppressed the abilities of Ad.5/3-*mda*-7 as well as 4HPR or 17AAG to promote CD95 activation and suppressed the induction of cytosolic Ca^{2+} and ROS by either 17AAG or 4HPR. Surprisingly, however, our data demonstrated that 17AAG did not significantly enhance bulk MDA-7/IL-24–induced ceramide or dihydro-ceramide levels. However, when ER stress signaling was compromised by expression of dominant-negative PERK that blocked the MDA-7/IL-24–induced increase in ceramide levels, 17AAG was able to partially overcome the block to ER stress signaling and facilitate MDA-7/IL-24–induced ceramide generation. Clearly, a more detailed time course analysis of ceramide generation and degradation pathways will be required to fully understand the interaction of 17AAG and MDA-7/IL-24 with respect to lipid signaling and how ceramide levels are regulated. Thus, our data argue that ceramide generation or alterations in ceramide metabolism caused by expression of MDA-7/IL-24 is essential for Ad.5/3-*mda*-7 lethality and for the ability of agents that generate ROS, such as 17AAG or 4HPR, to activate CD95 and to ultimately cause tumor cell killing (Fig. 7).

The actions of As_2O_3 (a therapeutic agent) in leukemic cells have largely been linked to the generation of ROS and the induction of tumor cell differentiation (Zhou et al., 2007). Unlike either 4HPR or 17AAG, As_2O_3 can degenerate to release arsenic as well as O^-; hence, its ability enhance MDA-7/IL-24 toxicity would be expected to have some differences from those of 4HPR or 17AAG. Indeed, unlike 4HPR or 17AAG, quenching of cytosolic Ca^{2+} or inhibition of de novo ceramide synthesis pathways did not prevent As_2O_3 from interacting with MDA-7/IL-24 to profoundly increase ROS levels. In addition, the reverse of our data with 4HPR or

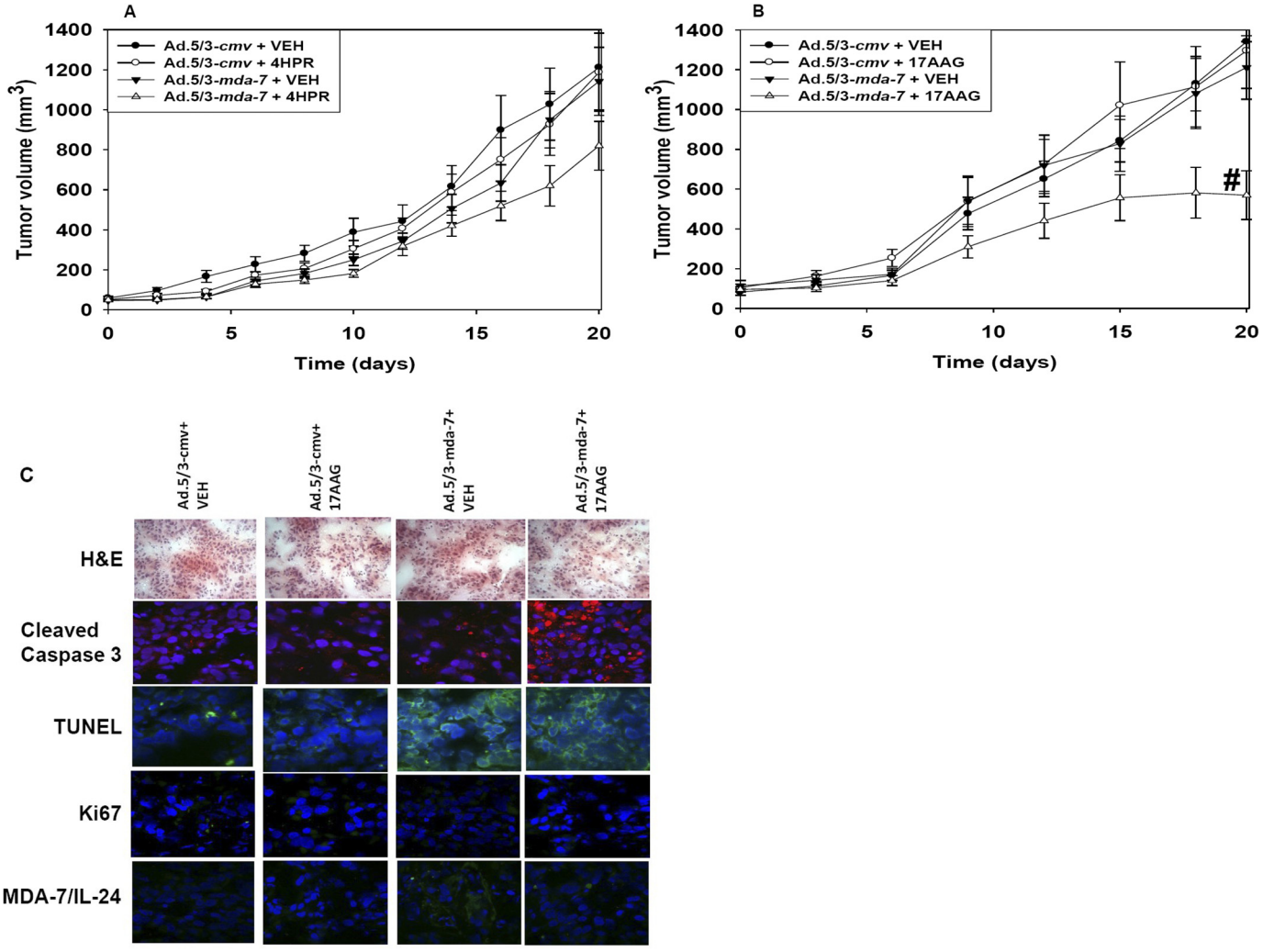

Fig. 6. Ad.5/3-*mda*-7 infection of RCC tumors suppresses RCC tumor growth that is enhanced by 17AAG. A and B, A498 cells were injected into the rear right flanks of athymic mice. Tumors were grown over the subsequent 29 days. Animals were segregated into tumor volumes of approximate equivalent mean tumor size and standard error; the tumor was injected with either Ad.5/3-*cmv* or Ad.5/3-*mda*-7. Animals were treated 24 h later with either vehicle or 4HPR (100 mg/kg) (A) or 17AAG (100 mg/kg) (B) every day for 3 days. One week after the first virus infection, tumors were again infected in an identical manner with adenovirus. Tumor volumes were measured every 2 or 3 days. The mean volume of the tumor is presented as a fold increase over the preinfected volume (defined as 1.00) ($n = 2$, ± S.E.M.; 9–10 mice per group total over two studies; #, $p < 0.05$ less than vehicle or individual treatments). C, A498 tumors were isolated 2 days after the second virus infection. Sections (10 μm) were taken and stained by hematoxylin and eosin (H&E; morphology) and TUNEL (apoptosis) and for cleaved caspase 3, Ki67, and MDA-7/IL-24 expression. Data are from representative images from multiple tumors shown for hematoxylin and eosin at 20× magnification and for other slides using a confocal microscope at 100× magnification.

17AAG with respect to changes in cytosolic Ca^{2+} was observed using As_2O_3; the As_2O_3-induced increase of Ca^{2+} was ROS-dependent. However, despite all of these differences and in a manner similar to 4HPR or 17AAG, and despite all of the additional ROS generation caused by As_2O_3 + Ad.5/3-*mda*-7 treatment, As_2O_3 still required CD95 expression/functionality and LASS6 function to enhance MDA-7/IL-24 lethality. Thus as with MDA-7/IL-24 itself, which can kill tumor cells through multiple convergent apoptotic mechanisms, agents that generate ROS can facilitate MDA-7/IL-24 lethality through multiple mechanisms that converge on enhanced death receptor signaling.

MDA-7/IL-24 is a secreted cytokine and has been shown in several studies to have a "toxic bystander" effect on distant tumor cells (Sarkar et al., 2002; Su et al., 2005; Sauane et al., 2008; Emdad et al., 2009; Eulitt et al., 2010 and references therein). We discovered that secreted MDA-7/IL-24 produces a conditioned media that, when placed onto uninfected RCCs, suppresses the growth of the uninfected cells and elevates apoptosis levels in a CD95–dependent fashion; this lethality is further enhanced by As_2O_3, 4HPR, and by 17AAG. Based on simple mass action effects, it is not possible to infect every tumor cell within a tumor using an adenovirus, and this has been one possible reason why so many gene therapy approaches have failed in the clinic. As MDA-7/IL-24 is secreted, our findings argue that this cytokine could have therapeutic utility in chemotherapy-resistant metastatic renal carcinoma. That a 20-fold lower Ad.5/3-*mda*-7 virus dose resulted in no significant alteration in tumor growth argues that for translation into the clinic to achieve optimal results, a virus with serotype modification plus tumor conditional replication in addition to MDA-7/IL-24 production and an approach to target virus delivery using systemic administration may be required (i.e., Ad.5/3-CTV) (Greco et al., 2010).

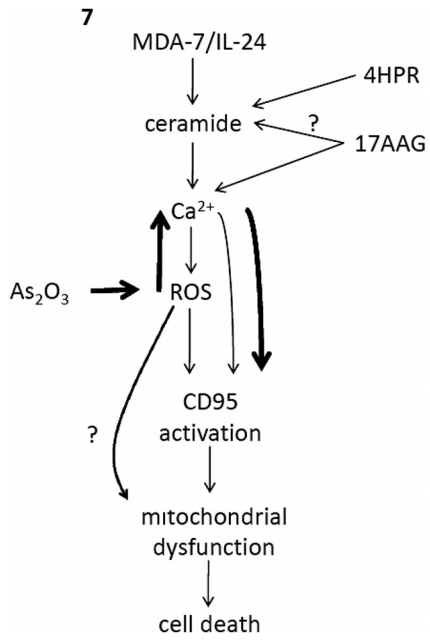

Fig. 7. Mechanisms by which agents that generate ROS interact with MDA-7/IL-24 to kill kidney cancer cells. As a single agent, MDA-7/IL-24 kills tumor cells by generating ceramide that in turn promotes elevation in cytosolic Ca^{2+} levels, which in turn promotes increased ROS levels. Increased ceramide (via lipid rafts), Ca^{2+}, and ROS by altering CD95 phosphorylation and through unknown mechanisms all also independently facilitate activation of CD95 (extrinsic pathway). Activation of the extrinsic pathway through caspase 8/BID cleavage causes kidney cancer cell killing by promoting mitochondrial dysfunction. The drugs 17AAG and 4HPR both enhance signaling proximal to MDA-7/IL-24 to "boost" the established MDA-7/IL-24 pro-apoptotic pathway. The drug As_2O_3 (heavier arrows) acts distally to ceramide resulting in increased ROS levels that increases Ca^{2+} levels, again with MDA-7/IL-24 –induced ceramide combining with elevated ROS and Ca^{2+} levels to activate CD95 and cause tumor cell killing.

One characteristic hallmark of RCC is loss of VHL protein expression (Ishizawa et al., 2004). We found that re-expression of VHL in VHL(−/−) RCCs suppressed MDA-7/IL-24 toxicity, in agreement with data arguing that VHL-expressing RCCs are less tumorigenic and that MDA-7/IL-24 toxicity is reduced in nontransformed cells. MDA-7/IL-24 kills tumor cells, in part, by causing a toxic form of ER stress, and one plausible mechanism for the disparity in MDA-7/IL-24 toxicity in transformed versus nontransformed cells is the greater levels of protein expression and unfolded proteins in transformed cells. Because VHL is an E3 ligase the actions of which will tend to reduce the toxic protein load in a tumor cell, our findings are also compatible with VHL expressing cells having a lower load of unfolded (toxic) proteins.

Prior studies from our laboratory have noted that MDA-7/IL-24 can suppress the growth of RCC tumors and has a bystander effect, an effect that can be enhanced by the multikinase inhibitor sorafenib (Eulitt et al., 2010). On the basis of the findings in the present manuscript, we attempted to determine whether agents that generate ROS could enhance MDA-7/IL-24 toxicity in RCC tumors. To our surprise, 4HPR did not seem to interact in vivo with MDA-7/IL-24 expression to suppress tumor growth rates. Clearly, further studies are required using higher doses of 4HPR and altered administration schedules to confirm this lack of in vivo effect. In contrast, 17AAG significantly reduced growth in tumors infected with Ad.5/3-*mda*-7. It is possible that the effect of 17AAG was due to generation of both ROS and to inhibition of protective signaling pathways in the tumors. Further studies, including the clinical translation of viruses to express MDA-7/IL-24 into patients, will be required to define potential therapeutic efficacy of MDA-7/IL-24 in kidney cancer.

Authorship Contributions

Participated in research design: Dent.

Conducted experiments: Park, Hamed, Cruickshanks, Dash, and Allegood.

Contributed new reagents or analytic tools: Dmitriev, Ogretmen, and Curiel.

Performed data analysis: Park, Hamed, Allegood, and Dent.

Wrote or contributed to the writing of the manuscript: Grant, Fisher, and Dent.

Other: Tye, Spiegel, and Yacoub supervised elements of experimentation and data analysis.

References

Azad MB, Chen Y, and Gibson SB (2009) Regulation of autophagy by reactive oxygen species (ROS): implications for cancer progression and treatment. *Antioxid Redox Signal* **11:**777–790.

Caudell EG, Mumm JB, Poindexter N, Ekmekcioglu S, Mhashilkar AM, Yang XH, Retter MW, Hill P, Chada S, and Grimm EA (2002) The protein product of the tumor suppressor gene, melanoma differentiation-associated gene 7, exhibits immunostimulatory activity and is designated IL-24. *J Immunol* **168:**6041–6046.

Cunningham CC, Chada S, Merritt JA, Tong A, Senzer N, Zhang Y, Mhashilkar A, Parker K, Vukelja S, Richards D, et al. (2005) Clinical and local biological effects of an intratumoral injection of *mda-7* (IL24; INGN 241) in patients with advanced carcinoma: a phase I study. *Mol Ther* **11:**149–159.

Dash R, Dmitriev I, Su ZZ, Bhutia SK, Azab B, Vozhilla N, Yacoub A, Dent P, Curiel DT, Sarkar D, et al. (2010) Enhanced delivery of mda-7/IL-24 using a serotype

chimeric adenovirus (Ad. 5/3) improves therapeutic efficacy in low CAR prostate cancer cells. *Cancer Gene Ther* **17:**447–456.
Ekmekcioglu S, Ellerhorst J, Mhashilkar AM, Sahin AA, Read CM, Prieto VG, Chada S, and Grimm EA (2001) Down-regulated melanoma differentiation associated gene (*mda-7*) expression in human melanomas. *Int J Cancer* **94:**54–59.
Ellerhorst JA, Prieto VG, Ekmekcioglu S, Broemeling L, Yekell S, Chada S, and Grimm EA (2002) Loss of MDA-7 expression with progression of melanoma. *J Clin Oncol* **20:**1069–1074.
Emdad L, Lebedeva IV, Su ZZ, Gupta P, Sauane M, Dash R, Grant S, Dent P, Curiel DT, Sarkar D, et al. (2009) Historical perspective and recent insights into our understanding of the molecular and biochemical basis of the antitumor properties of mda-7/IL-24. *Cancer Biol Ther* **8:**391–400.
Eulitt PJ, Park MA, Hossein H, Cruikshanks N, Yang C, Dmitriev IP, Yacoub A, Curiel DT, Fisher PB, and Dent P (2010) Enhancing mda-7/IL-24 therapy in renal carcinoma cells by inhibiting multiple protective signaling pathways using sorafenib and by Ad.5/3 gene delivery. *Cancer Biol Ther* **10:**1290–1305.
Fisher PB (2005) Is mda-7/IL-24 a "magic bullet" for cancer? *Cancer Res* **65**:10128–10138.
Fisher PB, Gopalkrishnan RV, Chada S, Ramesh R, Grimm EA, Rosenfeld MR, Curiel DT, and Dent P (2003) mda-7/IL-24, a novel cancer selective apoptosis inducing cytokine gene: from the laboratory into the clinic. *Cancer Biol Ther* **2**:S23–S37.
Gillett MD, Cheville JC, Karnes RJ, Lohse CM, Kwon ED, Leibovich BC, Zincke H, and Blute ML (2005) Comparison of presentation and outcome for patients 18 to 40 and 60 to 70 years old with solid renal masses. *J Urol* **173:**1893–1896.
Gopalan B, Litvak A, Sharma S, Mhashilkar AM, Chada S, and Ramesh R (2005) Activation of the Fas-FasL signaling pathway by MDA-7/IL-24 kills human ovarian cancer cells. *Cancer Res* **65:**3017–3024.
Greco A, Di Benedetto A, Howard CM, Kelly S, Nande R, Dementieva Y, Miranda M, Brunetti A, Salvatore M, Claudio L, et al. (2010) Eradication of therapy-resistant human prostate tumors using an ultrasound-guided site-specific cancer terminator virus delivery approach. *Mol Ther* **18:**295–306.
Gupta P, Emdad L, Lebedeva IV, Sarkar D, Dent P, Curiel DT, Settleman J, and Fisher PB (2008) Targeted combinatorial therapy of non-small cell lung carcinoma using a GST-fusion protein of full-length or truncated MDA-7/IL-24 with Tarceva. *J Cell Physiol* **215:**827–836.
Gupta P, Su ZZ, Lebedeva IV, Sarkar D, Sauane M, Emdad L, Bachelor MA, Grant S, Curiel DT, Dent P, et al. (2006) mda-7/IL-24: multifunctional cancer-specific apoptosis-inducing cytokine. *Pharmacol Ther* **111**:596–628.
Gupta P, Walter MR, Su ZZ, Lebedeva IV, Emdad L, Randolph A, Valerie K, Sarkar D, and Fisher PB (2006a) BiP/GRP78 is an intracellular target for MDA-7/IL-24 induction of cancer-specific apoptosis. *Cancer Res* **66:**8182–8191.
Hait NC, Allegood J, Maceyka M, Strub GM, Harikumar KB, Singh SK, Luo C, Marmorstein R, Kordula T, Milstien S, et al. (2009) Regulation of histone acetylation in the nucleus by sphingosine-1-phosphate. *Science* **325:**1254–1257.
Hamed HA, Yacoub A, Park MA, Eulitt PJ, Dash R, Sarkar D, Dmitriev IP, Lesniak MS, Shah K, Grant S, et al. (2010) Inhibition of multiple protective signaling pathways and Ad.5/3 delivery enhances mda-7/IL-24 therapy of malignant glioma. *Mol Ther* **18:**1130–1142.
Huang EY, Madireddi MT, Gopalkrishnan RV, Leszczyniecka M, Su Z, Lebedeva IV, Kang D, Jiang H, Lin JJ, Alexandre D, et al. (2001) Genomic structure, chromosomal localization and expression profile of a novel melanoma differentiation associated (*mda-7*) gene with cancer specific growth suppressing and apoptosis inducing properties. *Oncogene* **20:**7051–7063.
Ishizawa J, Yoshida S, Oya M, Mizuno R, Shinojima T, Marumo K, and Murai M (2004) Inhibition of the ubiquitin-proteasome pathway activates stress kinases and induces apoptosis in renal cancer cells. *Int J Oncol* **25:**697–702.
Jiang H, Lin JJ, Su ZZ, Goldstein NI, and Fisher PB (1995) Subtraction hybridization identifies a novel melanoma differentiation associated gene, *mda-7*, modulated during human melanoma differentiation, growth and progression. *Oncogene* **11:**2477–2486.
Lai WL and Wong NS (2008) The PERK/eIF2 alpha signaling pathway of Unfolded Protein Response is essential for N-(4-hydroxyphenyl)retinamide (4HPR)-induced cytotoxicity in cancer cells. *Exp Cell Res* **314:**1667–1682.
Lebedeva IV, Emdad L, Su ZZ, Gupta P, Sauane M, Sarkar D, Staudt MR, Liu SJ, Taher MM, Xiao R, et al. (2007a) mda-7/IL-24, novel anticancer cytokine: focus on bystander antitumor, radiosensitization and antiangiogenic properties and overview of the phase I clinical experience (review). *Int J Oncol* **31:**985–1007.
Lebedeva IV, Sauane M, Gopalkrishnan RV, Sarkar D, Su ZZ, Gupta P, Nemunaitis J, Cunningham C, Yacoub A, Dent P, et al. (2005) mda-7/IL-24: exploiting cancer's Achilles' heel. *Mol Ther* **11**:4–18.
Lebedeva IV, Su ZZ, Chang Y, Kitada S, Reed JC, and Fisher PB (2002) The cancer growth suppressing gene *mda-7* induces apoptosis selectively in human melanoma cells. *Oncogene* **21:**708–718.
Lebedeva IV, Su ZZ, Sarkar D, Gopalkrishnan RV, Waxman S, Yacoub A, Dent P, and Fisher PB (2005a) Induction of reactive oxygen species renders mutant and wild-type K-ras pancreatic carcinoma cells susceptible to Ad.mda-7-induced apoptosis. *Oncogene* **24:**585–596.
Lebedeva IV, Washington I, Sarkar D, Clark JA, Fine RL, Dent P, Curiel DT, Turro NJ, and Fisher PB (2007b) Strategy for reversing resistance to a single anticancer agent in human prostate and pancreatic carcinomas. *Proc Natl Acad Sci USA* **104:**3484–3489.
Mitchell C, Park MA, Zhang G, Han SI, Harada H, Franklin RA, Yacoub A, Li PL, Hylemon PB, Grant S, et al. (2007) 17-Allylamino-17-demethoxygeldanamycin enhances the lethality of deoxycholic acid in primary rodent hepatocytes and established cell lines. *Mol Cancer Ther* **6:**618–632.
Park MA, Mitchell C, Zhang G, Yacoub A, Allegood J, Häussinger D, Reinehr R, Larner A, Spiegel S, Fisher PB, et al. (2010) Vorinostat and sorafenib increase CD95 activation in gastrointestinal tumor cells through a Ca^{2+}-de novo ceramide-PP2A-reactive oxygen species-dependent signaling pathway. *Cancer Res* **70:**6313–6324.
Park MA, Walker T, Martin AP, Allegood J, Vozhilla N, Emdad L, Sarkar D, Rahmani M, Graf M, Yacoub A, et al. (2009) MDA-7/IL-24-induced cell killing in malignant renal carcinoma cells occurs by a ceramide/CD95/PERK-dependent mechanism. *Mol Cancer Ther* **8:**1280–1291.
Park MA, Zhang G, Mitchell C, Rahmani M, Hamed H, Hagan MP, Yacoub A, Curiel DT, Fisher PB, Grant S, et al. (2008) Mitogen-activated protein kinase kinase 1/2 inhibitors and 17-allylamino-17-demethoxygeldanamycin synergize to kill human gastrointestinal tumor cells in vitro via suppression of c-FLIP-s levels and activation of CD95. *Mol Cancer Ther* **7:**2633–2648.
Parrish-Novak J, Xu W, Brender T, Yao L, Jones C, West J, Brandt C, Jelinek L, Madden K, McKernan PA, et al. (2002) Interleukins 19, 20, and 24 signal through two distinct receptor complexes. Differences in receptor-ligand interactions mediate unique biological functions. *J Biol Chem* **277:**47517–47523.
Pestka S, Krause CD, Sarkar D, Walter MR, Shi Y, and Fisher PB (2004) Interleukin-10 and related cytokines and receptors. *Annu Rev Immunol* **22:**929–979.
Sarkar D, Su ZZ, Lebedeva IV, Sauane M, Gopalkrishnan RV, Valerie K, Dent P, and Fisher PB (2002) mda-7 (IL-24) Mediates selective apoptosis in human melanoma cells by inducing the coordinated overexpression of the GADD family of genes by means of p38 MAPK. *Proc Natl Acad Sci USA* **99:**10054–10059.
Sauane M, Gopalkrishnan RV, Choo HT, Gupta P, Lebedeva IV, Yacoub A, Dent P, and Fisher PB (2004a) Mechanistic aspects of mda-7/IL-24 cancer cell selectivity analysed via a bacterial fusion protein. *Oncogene* **23:**7679–7690.
Sauane M, Lebedeva IV, Su ZZ, Choo HT, Randolph A, Valerie K, Dent P, Gopalkrishnan RV, and Fisher PB (2004b) Melanoma differentiation associated gene-7/interleukin-24 promotes tumor cell-specific apoptosis through both secretory and nonsecretory pathways. *Cancer Res* **64:**2988–2993.
Sauane M, Su ZZ, Dash R, Liu X, Norris JS, Sarkar D, Lee SG, Allegood JC, Dent P, Spiegel S, et al. (2010) Ceramide plays a prominent role in MDA-7/IL-24-induced cancer-specific apoptosis. *J Cell Physiol* **222:**546–555.
Sauane M, Su ZZ, Gupta P, Lebedeva IV, Dent P, Sarkar D, and Fisher PB (2008) Autocrine regulation of mda-7/IL-24 mediates cancer-specific apoptosis. *Proc Natl Acad Sci USA* **105:**9763–9768.
Su Z, Emdad L, Sauane M, Lebedeva IV, Sarkar D, Gupta P, James CD, Randolph A, Valerie K, Walter MR, Dent P, and Fisher PB (2005) Unique aspects of mda-7/IL-24 antitumor bystander activity: establishing a role for secretion of MDA-7/IL-24 protein by normal cells. *Oncogene* **24:**7552–7566.
Su Z, Lebedeva IV, Gopalkrishnan RV, Goldstein NI, Stein CA, Reed JC, Dent P, and Fisher PB (2001) A combinatorial approach for selectively inducing programmed cell death in human pancreatic cancer cells. *Proc Natl Acad Sci USA* **98:**10332–10337.
Su ZZ, Lebedeva IV, Sarkar D, Emdad L, Gupta P, Kitada S, Dent P, Reed JC, and Fisher PB (2006) Ionizing radiation enhances therapeutic activity of mda-7/IL-24: overcoming radiation- and mda-7/IL-24-resistance in prostate cancer cells overexpressing the antiapoptotic proteins bcl-xL or bcl-2. *Oncogene* **25:**2339–2348.
Su ZZ, Madireddi MT, Lin JJ, Young CS, Kitada S, Reed JC, Goldstein NI, and Fisher PB (1998) The cancer growth suppressor gene *mda-7* selectively induces apoptosis in human breast cancer cells and inhibits tumor growth in nude mice. *Proc Natl Acad Sci USA* **95:**14400–14405.
Turcotte S, Chan DA, Sutphin PD, Hay MP, Denny WA, and Giaccia AJ (2008) A molecule targeting VHL-deficient renal cell carcinoma that induces autophagy. *Cancer Cell* **14:**90–102.
Yacoub A, Gupta P, Park MA, Rhamani M, Hamed H, Hanna D, Zhang G, Sarkar D, Lebedeva IV, Emdad L, et al. (2008a) Regulation of GST-MDA-7 toxicity in human glioblastoma cells by ERBB1, ERK1/2, PI3K, and JNK1–3 pathway signaling. *Mol Cancer Ther* **7:**314–329.
Yacoub A, Hamed HA, Allegood J, Mitchell C, Spiegel S, Lesniak MS, Ogretmen B, Dash R, Sarkar D, Broaddus WC, et al. (2010) PKR endoplasmic reticulum kinase dependent regulation of ceramide synthase 6 and thioredoxin controls melanoma differentiation associated gene-7 glioma cell killing. *Cancer Res* **70:**1120–1129.
Yacoub A, Mitchell C, Brannon J, Rosenberg E, Qiao L, McKinstry R, Linehan WM, Su ZS, Sarkar D, Lebedeva IV, et al. (2003) MDA-7 (interleukin-24) inhibits the proliferation of renal carcinoma cells and interacts with free radicals to promote cell death and loss of reproductive capacity. *Mol Cancer Ther* **2:**623–632.
Yacoub A, Park MA, Gupta P, Rahmani M, Zhang G, Hamed H, Hanna D, Sarkar D, Lebedeva IV, Emdad L, et al. (2008b) Caspase-, cathepsin-, and PERK-dependent regulation of MDA-7/IL-24-induced cell killing in primary human glioma cells. *Mol Cancer Ther* **7:**297–313.
Zhou GB, Zhang J, Wang ZY, Chen SJ, and Chen Z (2007) Treatment of acute promyelocytic leukaemia with all-trans retinoic acid and arsenic trioxide: a paradigm of synergistic molecular targeting therapy. *Philos Trans R Soc Lond B Biol Sci* **362:**959–971.

Address correspondence to: Paul Dent, 401 College Street, Massey Cancer Center, Box 980035, Department of Neurosurgery, Virginia Commonwealth University, Richmond VA 23298-0035. E-mail: pdent@vcu.edu.